nature communications

Article

https://doi.org/10.1038/s41467-026-75601-9

Thermomechanically squeezed multi-mode phonon lasers with levitated optomechanics

Received: 7 January 2026

Accepted: 6 July 2026

Published online: 14 July 2026

Check for updates

Xintao Song[1,2], Guoyao Li[1,2], Tengfang Kuang[1,2], Ran Huang[3], Wei Xiong[1,2], Xinlin Chen[1,2], Xiang Han[1,2], Yang Zhang[1,2], Franco Nori[3,4], Hui Jing[5], Hui Luo[1,2] & Guangzong Xiao[1,2]

Squeezing, an effective approach to reduce noise in one quadrature while increasing it in the orthogonal quadrature, has attracted broad attention to enhance the performance of mechanical oscillators in their thermal or ground states. However, the classical squeezing of phonon lasers, mechanical analogs of optical lasers, has not been achieved. Here, we report an experimental demonstration of a thermomechanically squeezed phonon laser with a microscale sphere in a levitated optomechanical system. Through non-adiabatic frequency shifts induced by a pulse-modulated trapping laser, the fundamental-mode phonon laser has been squeezed by 3.15 ± 0.35 dB. In such a way, we found that the second-harmonic mode of phonon lasers could be simultaneously squeezed, demonstrating the unique advantage of our system for concurrent coherent control of multi-mode phonon lasers. This work gives the first example of a squeezed nonlinear phonon laser with a larger mass under low vacuum, thus providing a promising platform for exploring non-linear phononics and harnessing such a system for precision metrology.

Phonon lasers, self-sustained motion of mechanical oscillators[1,2], are regarded as valuable resources for practical applications in precision metrology[3–5] and informatics[2], as well as fundamental research in thermodynamics[6,7] and non-Hermitian physics[8–10]. They have been realized in trapped ions[1,11], levitated spheres[12,13], membranes[14,15], microresonators[16–20], and nanobeams[21,22], characterized by three symbolic hallmarks including threshold behavior, linewidth narrowing, and second-order coherence approaching unity[12]. In recent years, diverse technologies have been developed for improving the phonon lasers, including injection locking[23–27], self-organized synchronization[2], and Floquet engineering[28,29]. These breakthroughs enable further advancement of metrology (e.g., force sensing) with phonon lasers.

Mechanical squeezing, suppressing momentum (position) noise at the cost of increased noise in the orthogonal quadrature, provides an effective method to enhance the performance of phonon lasers. Recently, classical squeezing has been implemented in a variety of systems with distinct mechanical resonators, such as clamped cantilevers[30], soft-clamped membranes[31–33], and levitated spheres[34–37], a detailed parameter comparison is in Supplementary Note 1. Due to the absence of mechanical contact with the thermal environment, levitated spheres in vacuum are expected to be ideal platforms for precision sensing. A classical squeezing of 2.7 dB has been achieved in a thermal nanosphere[34]. Further squeezing in the same system has demonstrated a frontier exploration of inherent Duffing nonlinearities[37]. However, squeezing a levitated sphere in the multi-mode phonon lasing state remains unexplored and is even more difficult for larger spheres due to low oscillating frequencies[31,38,39]

In this work, for the first time, we demonstrate the squeezed phonon lasers of both the fundamental mode and nonlinear higher-order harmonics with microspheres. Notably, compared with previous works[41], our approach operates with a large phonon number (~ 10^{10}) of micro-sized spheres. Even under massive thermal fluctuations, the

[1]College of Advanced Interdisciplinary Studies, National University of Defense Technology, Changsha, China. [2]Nanhu Laser Laboratory, National University of Defense Technology, Changsha, China. [3]Quantum Information Physics Theory Research Team, Center for Quantum Computing (RQC), RIKEN, Wakoshi Saitama, Japan. [4]Physics Department, University of Michigan, Ann Arbor, MI, USA. [5]Institute for Quantum Science and Technology, College of Science, National University of Defense Technology, Changsha, China. e-mail: jinghui@hunnu.edu.cn; luohui.luo@163.com; xiaoguangzong@nudt.edu.cn

thermal noise of the nonlinear phonon lasers is suppressed effectively, yielding a maximum squeezing of 3.15 ± 0.35 dB for the fundamental mode and 1.23 ± 0.17 dB for the second-harmonic mode. Moreover, our active system can provide strong mechanical gain, and thus has the ability to squeeze a microscale sphere without the challenging requirement of high vacuum[32].

Results

Experimental setup and principle

Our experimental apparatus includes an active optical cavity and dual-beam optical tweezers, as illustrated in Fig. 1a (see Methods for more details). More specifically, a microsphere (diameter ~2 µm) is trapped in a vacuum chamber (~20 mbar), interacting with the active cavity through dissipative coupling[40]. The quality factor of this cavity is enhanced to 10^9 by incorporating a Yb^{3+}-doped gain fiber, extending the photon lifetime and allowing coherent vibrational amplification of the microsphere. By increasing the pump power P of this active cavity beyond a threshold, the microsphere undergoes a phase transition from thermal motion to sustained coherent oscillation. The phase transition has also been observed in various non-Hermitian systems, which are typically passive and rely on non-reciprocal coupling[41,42]. In contrast, our system is active and operates in the dissipative coupling regime, requiring no complicated external feedback. Furthermore, in our previous work, we explored the ability of the active cavity to drive high-order mechanical harmonics, known as nonlinear phonon lasers[13], resulting from the optical-gain-enhanced nonlinearity.

Here, an approach based on non-adiabatic frequency shifts is employed. The introduced interaction $(\hat{b}^{\dagger 2}+\hat{b}^2)$ will drive the phonon laser to squeezing[43–48]. We employed an acousto-optic modulator (AOM) to control the power of the trapping beam, enabling non-adiabatic frequency tunability of the phonon laser. A short squeezing pulse with duration τ is applied by switching between two different trapping powers P_1 (350 mW) and P_2 (55 mW), corresponding to the phonon laser frequencies Ω_1 (2π × 17.8 kHz) and Ω_2 (2π × 7.1 kHz), see Fig. 1b. The dimensionless Hamiltonians are given as $\hat{H}_1=\hbar\Omega_1(\hat{b}_1^{\dagger}\hat{b}_1+1/2)$ and $\hat{H}_2=\hbar\Omega_2(\hat{b}_2^{\dagger}\hat{b}_2+1/2)$, where the operators $\hat{b}_1^{\dagger}(\hat{b}_2^{\dagger})$ and $\hat{b}_1(\hat{b}_2)$ are the creation and annihilation operators. Due to the non-ideal response of the AOM, there are rising and falling edges Δt on modulated optical pulses (Fig.1b). If the time scale Δt satisfies the non-adiabatic condition ($\Delta t \ll \Omega_{1,2}$), the induced squeezing interaction will suppress the noise of a specific quadrature while amplifying the noise of its orthogonal quadrature[49,50] (more details in Supplementary Note 2).

Immediately after the sudden change, the creation and annihilation operators satisfy the Bogoliubov transformation[44,47]:

$$\begin{aligned}\hat{b}_2^{\dagger} &= \cosh(r)\hat{b}_1^{\dagger}+\sinh(r)\hat{b}_1 e^{i\theta}=\hat{S}(r)\hat{b}_1^{\dagger}\hat{S}^{\dagger}(r),\\ \hat{b}_2 &= \cosh(r)\hat{b}_1+\sinh(r)\hat{b}_1^{\dagger}e^{i\theta}=\hat{S}^{\dagger}(r)\hat{b}_1\hat{S}(r),\end{aligned} \tag{1}$$

where $\hat{S}(\xi)=\exp[(\xi^*\hat{b}_1^2-\xi\hat{b}_1^{\dagger 2})/2]$ is the squeezing operator, $\xi = re^{i\theta}$ denotes the squeezing parameter, $r = \ln(\Omega_1/\Omega_2)/2$ is the squeezing magnitude, and θ is the squeezing angle. The theoretical squeezing degree is quantified in decibels (dB), defined as

$$\lambda = -10\log_{10}\exp(-r)=5\log_{10}\frac{\Omega_1}{\Omega_2}. \tag{2}$$

Therefore, the fluctuations in one quadrature are reduced below that of the initial state, while the fluctuations in the orthogonal quadrature are anti-squeezed, as depicted in Fig.1c. In our squeezing protocol, each square-wave pulse generates two distinct squeezing events. During the pulse, the oscillator's phase-space distribution rotates at Ω_2 continuously. Maximum squeezing is achieved when the pulse duration τ is set to $\pi/2\Omega_2$, as this allows the two squeezing effects to add constructively[35].

Squeezing of the fundamental mode

Figure 1d presents the experimental results of the squeezing and anti-squeezing processes for the fundamental-mode phonon lasers. We use the measured ratio σ^2_t/σ^2_0 to evaluate the degree of squeezing, where σ^2_0 is the mean value of the momentum noise variance before the pulse and σ^2_t denotes the variance at time t. Before the pulse, the ratio σ^2_t/σ^2_0 fluctuates slightly around 1, indicating no squeezing. Right after the pulse, the ratio σ^2_t/σ^2_0 shows a significant change, and its time evolution performs an underdamped oscillation around 1, owing to the decoherence induced by thermal noise. Specifically, the quadrature of the momentum noise undergoes squeezing and anti-squeezing, corresponding to $\sigma^2_t/\sigma^2_0 < 1$ (red) and $\sigma^2_t/\sigma^2_0 > 1$ (gray), respectively. After approximately 3 ms, the squeezing is ultimately annihilated by thermal fluctuations, and σ^2_t/σ^2_0 returns to the initial value. The insets of the phase space in Fig.1d exhibit the initial and squeezed states, corresponding to the evolution schematically shown in Fig. 1c.

The dynamics of the position and momentum quadratures for the squeezing and anti-squeezing processes are depicted in Fig. 2a. The dynamical phase spaces of four typical times are obtained from the position and momentum quadratures. Right after the pulse at $t = 0$ µs, the squeezed phonon lasers exhibit an elliptical limit cycle in phase space. The corresponding noise distribution becomes a solid ellipse. These results indicate that the noise levels of the position and momentum are no longer equal, leading to squeezing and anti-squeezing of these two quadratures. When time evolves, the phase of the microsphere undergoes a clockwise rotation with a period $T_1 = 2\pi/\Omega_1$. Throughout this evolution, the distribution gradually relaxes back to its initial state due to the stochastic collisions of the background gas.

We further investigate the ratio $\sigma^2_t/\sigma^2_0$and the normalized correlation function $g^{(2)}(0)$ (at zero-time delay) from the perspective of the pulse duration τ and trapping power ratio P_1/P_2, as shown in Fig. 2b and 2c, respectively. The ratio σ^2_t/σ^2_0 first decreases and then increases as the pulse width τ increases, and a maximum squeezing degree of 3.15 ± 0.35 dB ($\sigma^2_t/\sigma^2_0 \approx 0.484$) is achieved for $\tau_{\max} = T_2/4 \approx 35.53$ µs. We note that such a value of $\tau_{\max}$ corresponds to a squeezing angle of $\pi/2$, where the squeezing parameter $\xi = re^{i\theta}$ reaches its maximum, leading to the optimal squeezing. Moreover, the correlation function $g^{(2)}(0)$ is introduced to illustrate clear evidence of squeezing in these phonon lasers. As shown in Fig. 2b, $g^{(2)}(0)$ is nearly insensitive ($g^{(2)}(0) \approx 1$) to the pulse width τ, indicating that phonon coherence is preserved over the pulse duration.

Figure 2c shows the measured ratio σ^2_t/σ^2_0 and $g^{(2)}(0)$ as a function of the power ratio P_1/P_2. According to Eq. (2), the squeezing degree is determined by the ratio Ω_1/Ω_2, which involves the power ratio P_1/P_2. For convenience, we maintained P_1 constant and reduced P_2. Results show that a higher P_1/P_2 would lead to a reduction of σ^2_t/σ^2_0, which is in agreement with the theoretical prediction in Eq. (2). However, the correlation function $g^{(2)}(0)$ exhibits a sharp increase above the threshold (vertical dashed line in Fig. 2c), indicating that the coherence is not retained. We attribute this phenomenon to the position shift at excessively low P_2 (more details in Supplementary Note 3).

Squeezing of the second harmonic

Without loss of generality, the non-adiabatic frequency shifts enable us to squeeze the high-order mechanical modes. During the pulse modulation, the frequency of the second-harmonic mode jumps between $2\Omega_1$ and $2\Omega_2$, following the frequency switching of the fundamental mode. In Fig. 3a, we show the time evolution of the second-harmonic mode (2π × 35.6 kHz) in phase space, obtained with a pulse duration of $T_2/8$. The phase-space distributions at 0 µs and 7 µs exhibit the characteristic features of momentum squeezing and position squeezing,

https://doi.org/10.1038/s41467-026-75601-9

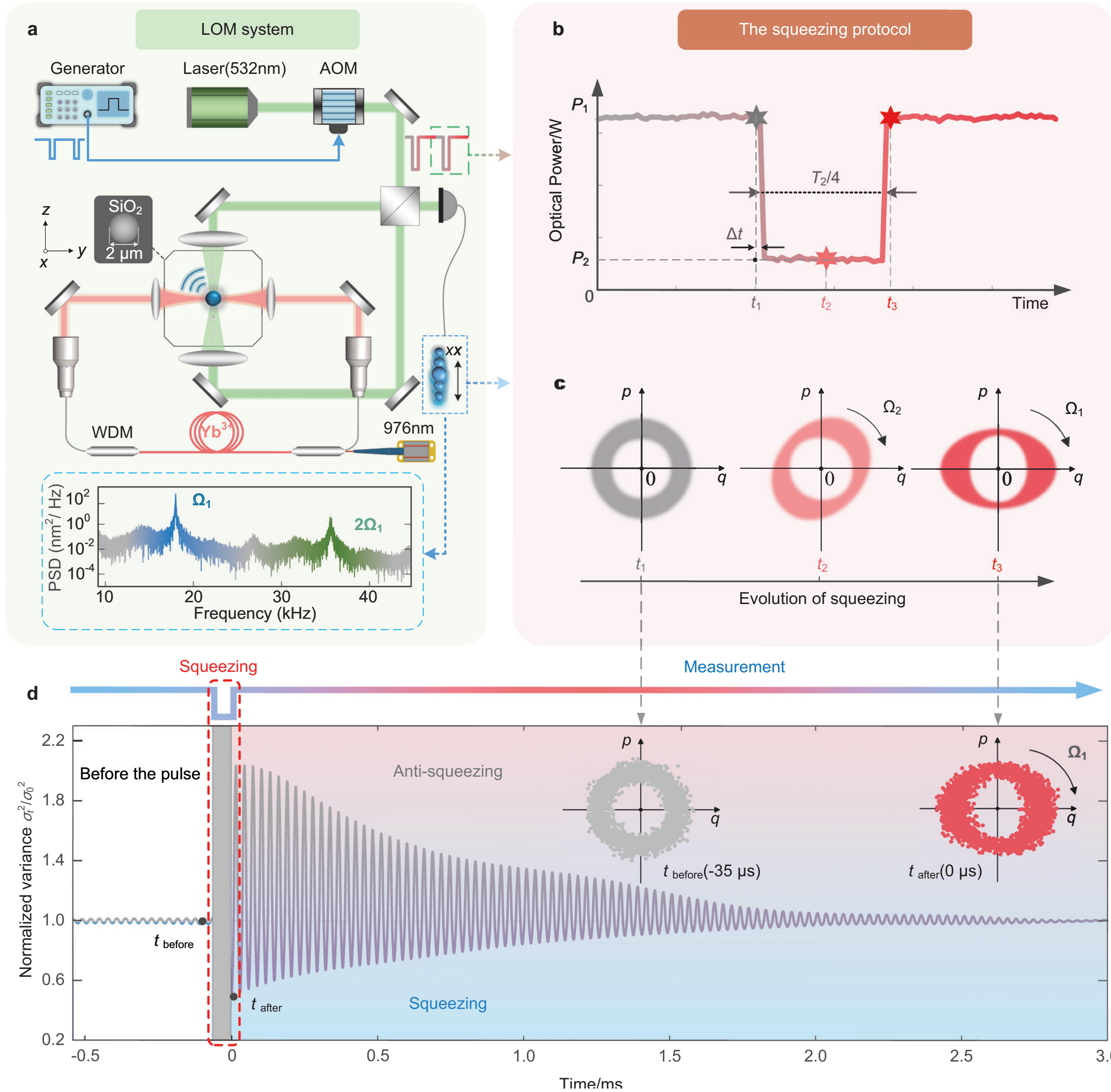

Fig. 1 | Experimental implementation of squeezed phonon lasers. a Schematic of the experimental setup for nonlinear phonon lasers squeezing. Trapping beams (green) trap a silica microsphere in vacuum (~ 20 mbar), with the inset at the bottom displaying the fundamental lasing mode Ω_1 and its second-harmonic mode $2\Omega_1$. The signal (blue) drives the AOM to change the power of the trapping beams, squeezing the nonlinear phonon lasers via nonadiabatic modulation. **b** Optical power of the trapping beam modulated by the AOM. **c** Schematic diagram of the phase-space distribution evolution during squeezing, where q and p denote the position quadrature and momentum quadrature, respectively. **d** Experimentally measured ratio σ^2_t/σ^2_0 undergoes squeezing and anti-squeezing, where σ^2_0 is the momentum noise variance before the pulse, and σ^2_t is calculated from the scatter points in the noise distributions at time t. The insets show the initial (left) and thermomechanically squeezed phonon laser (right), corresponding to the moments before and after the pulse, respectively.

respectively. This squeezing effect is manifested as a narrowed width of the limit cycle in the corresponding quadrature, making its trajectory approximate an ideal arc in phase space. Due to the thermal fluctuations, the squeezing effect decays completely within 0.8 ms after the pulse, as shown in Fig. 3b.

In Fig. 3c we further examine in more detail the normalized momentum noise variance σ^2_t/σ^2_0 with pulse duration τ and show the normalized correlation function $g^{(2)}(0)$. The ratio σ^2_t/σ^2_0 shows a periodic fluctuation with two minimum values. The noise distribution of the second-harmonic mode is squeezed and rotated in phase space, which means that there are optimal matching conditions between this rotation speed and the pulse widths τ for stronger squeezing. We note that the optimal pulse width τ is $\tau = (2n-1)T_2/8$ ($n = 1, 2$) in our system, where a minimum value of $\sigma^2_t/\sigma^2_0 \approx 0.753$ was measured with squeezing degree $\lambda \approx 1.23 \pm 0.17$ dB. In addition, $g^{(2)}(0)$ remains nearly unchanged (~1.2) across the pulse widths, indicating that the phonon coherence of the second-harmonic mode is inferior to that of the fundamental mode. In our work, both the fundamental and second-harmonic modes are squeezed simultaneously in the same measurement. For example, at the pulse width of $\tau \approx 18$ μs, we observe a squeezing of 1.67 ± 0.21 dB for the fundamental mode and 1.23 ± 0.17 dB for the second-harmonic mode, as shown in Figs. 2b and 3c. However, the optimal squeezing for each mode occurs at different pulse widths ($\tau = nT_2/4$ for the fundamental and $\tau = (2n-1)T_2/8$ for the second harmonic).

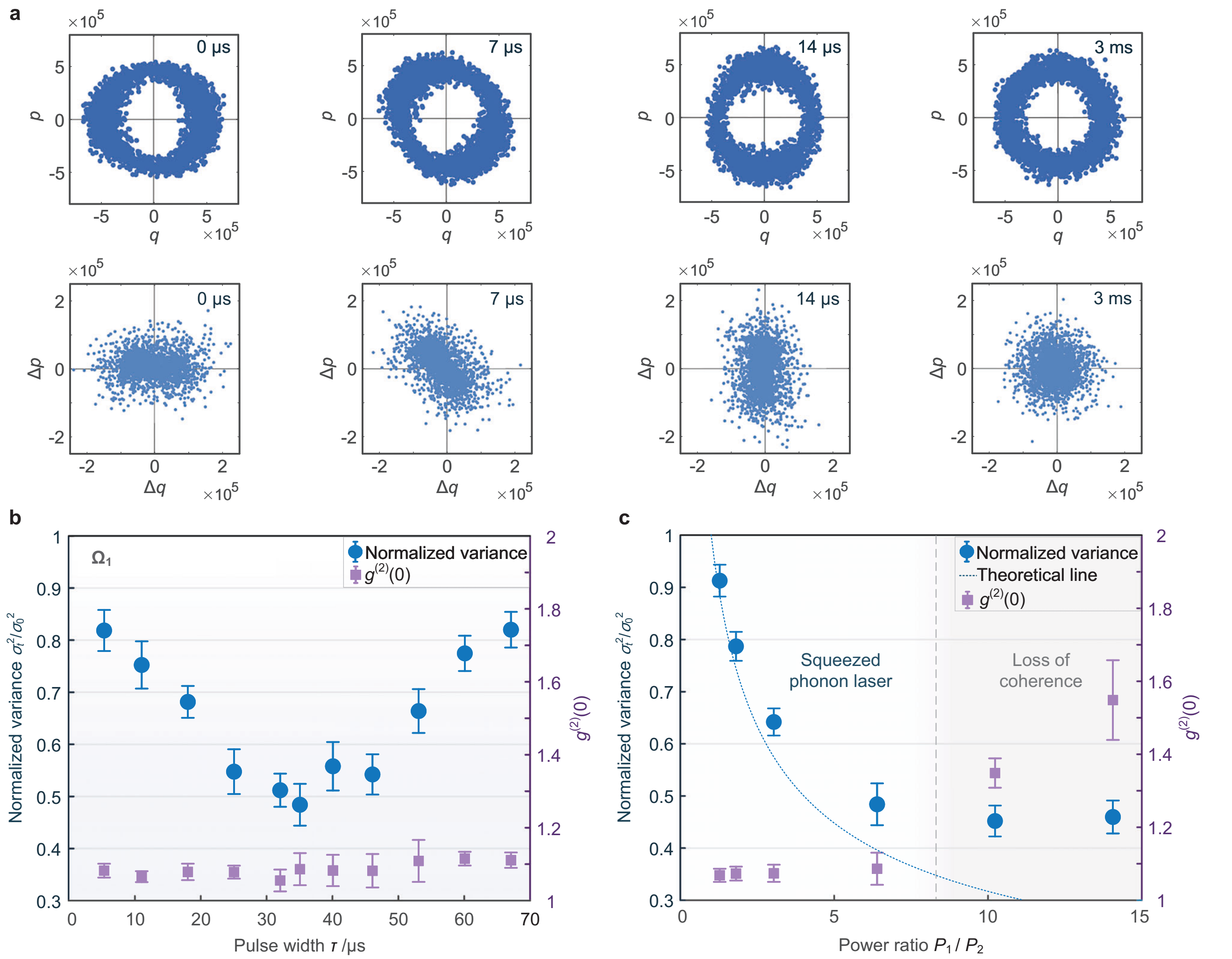

Fig. 2 | Squeezed nonlinear phonon lasers of the fundamental mode. a Variation of phase space after the squeezing protocol. Phase-space distributions (top) and noise distributions (bottom) of the microsphere, with the average amplitude of the phonon lasers subtracted. Here, q, p are the position, normalized by $\sqrt{\hbar/(2m\Omega)}$, and the momentum, normalized by $\sqrt{\hbar m\Omega/2}$. **b** The minimum value of the normalized variance varies with the pulse width τ, demonstrating one full cycle of its evolution. The maximum squeezing reaches 3.15 ± 0.35 dB when the pulse width equals $T_2/4$. **c** The ratio σ^2_τ/σ^2_0 and correlation function $g^{(2)}(0)$ versus the optical power ratio P_1/P_2. The blue decreasing dotted curve shows the theoretical expectation of σ^2_τ/σ^2_0 based on Eq. (2).

Note that our results are essentially different from those in a very recent experiment on quantum squeezing, where a levitated nanosphere was precooled to the quantum ground state[51,52]. In contrast, we drive a levitated microsphere from thermal behavior into a regime of sustained coherent oscillation, i.e., phonon lasing, and realize the thermomechanically squeezed phonon lasers, providing a new platform for advancing the performance of coherent phonon sources. In addition, we employ microspheres with larger mass, which exhibit significant dissipative optomechanical coupling and robustness against thermal noise[13]. This combination enables the effective squeezing of phonon lasers under conditions of low vacuum (~20 mbar), which is much higher than in the usual mechanical squeezing experiment[43–47].

Compared with previous demonstrations of mechanical squeezing[32], a key advantage of our system lies in its capability to simultaneously squeeze multiple mechanical modes of nonlinear phonon lasers, establishing the foundation for parallel sensing protocols across multiple degrees of freedom. In our future work, by further combining with other existing techniques used in previous studies[23,32,35,53], it is possible to achieve stronger squeezing, allowing studies of fundamental problems in nonequilibrium dynamics, mesoscopic classical thermodynamics[42] as well as tasks on ultrasensitive metrology[48,54].

Discussion

In conclusion, we report the first demonstration of a thermomechanically squeezed nonlinear phonon laser in an active levitated optomechanical system. Simultaneous squeezing of the fundamental and second-harmonic modes of the nonlinear phonon lasers is demonstrated, arising from the combination of non-adiabatic parameter control, optical-gain-enhanced nonlinearity, and dissipative engineering. We show that this platform could generate squeezing with microscale spheres under very desirable conditions (of both room temperature and low vacuum).

We suppress the momentum noise of the nonlinear phonon lasers, yielding a maximum squeezing degree of 3.15 ± 0.35 dB for the fundamental mode and 1.23 ± 0.17 dB for the second-harmonic mode, respectively. We note that squeezed light has played a breakthrough role in precision metrology, such as in gravitational-wave detection[55]. Similarly, squeezed phonon lasers are expected to play an important role in mass detection[56] and force sensing (electric fields[57,58], magnetic field[59], etc.). A canonical trapped-ion experiment illustrates the

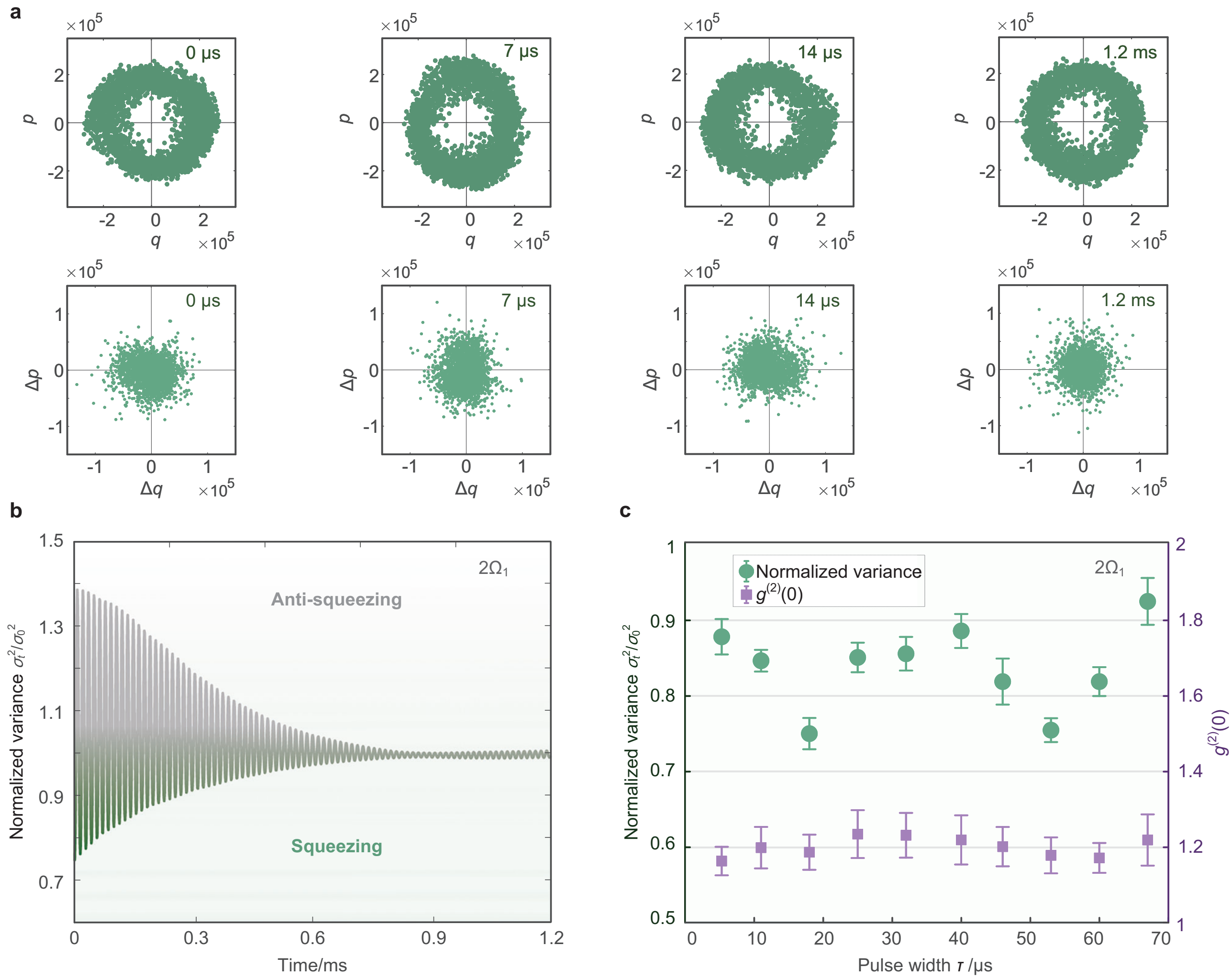

Fig. 3 | Squeezed second harmonic mode of the nonlinear phonon laser. **a** Measured phase-space distributions of the second harmonic mode after the pulse, showing (top) the phase-space of the microsphere and (bottom) the corresponding noise distributions, with the average amplitude of the phonon lasers subtracted. The rotation speed of the entire phase space is Ω_2. **b** Normalized variance of the microsphere momentum noise as a function of time, obtained from around 3000 pulse sequences. **c** The normalized variance as a function of the pulse width. Two minimum values are observed at pulse widths of $T_2/8$ and $3\,T_2/8$.

superior sensitivity of phonon lasers for detecting ultraweak electric forces F_e (~ 5 yN), with clear evidence that the sensitivity is ultimately limited by phase noise[23]. With the help of our squeezing method, we foresee that the sensitivity can be further improved by 3 dB. This improvement offers a complementary pathway beyond what is achievable with unsqueezed phonon lasers alone.

Moreover, our work also guides the future exploration of thermomechanically squeezed phonon laser combs. Combined with injection locking[23,24] and Floquet engineering[28,29], such multi-frequency squeezed phonon sources enable parallel sensing across multiple channels and enhance the dynamic range[59–61], which are difficult to achieve with a single-frequency squeezed phonon laser. We anticipate that our findings can be applied to boost nonlinear phononics and non-equilibrium physics, as well as applications in metrology.

Note added in proof: When submitting our revised manuscript, an experiment appeared, and in that work, a two-mode thermomechanically squeezed phonon laser has been demonstrated with a levitated nanoparticle in high vacuum[62]. Our work instead shows single-mode squeezing of both the fundamental and second harmonic modes of a nonlinear phonon laser with a larger microsphere. The two results are complementary, setting the stage for research on non-equilibrium physics and applications in precision metrology.

Methods

Experimental details

In our experiment, we employ a dual-beam optical tweezer and an active cavity, with the two setups arranged orthogonally to each other around the trapping region, as illustrated in Fig. 1a. For the dual-beam optical tweezer system, two orthogonally polarized beams (532 nm) are focused through opposing objective lenses (L Plan Fluor EPI 50×, NA = 0.5) to trap a silica microsphere in vacuum. The microsphere's position is monitored using a balanced differential detector that collects forward-scattered light[63]. Our vacuum chamber is placed between two objective lenses and features four coated optical windows (each 12.7 mm in diameter) on its four sides, which ensure high stability and low optical loss.

The active cavity consists of a Yb^{3+}-doped gain fiber, a pump laser (976 nm), and a free-space optical setup. Under optical pumping, the gain medium in the fiber undergoes stimulated emission, producing laser emission centered at 1030 nm. The clockwise and counter-clockwise propagating beams within the ring cavity are separately focused onto the microsphere using two collimating objective lenses (NA = 0.25). We position a microsphere within the active optical cavity by synchronously translating the objective lenses.

Compared with conventional optomechanical systems based on dispersive coupling, the active cavity here enables a direct channel for dissipative coupling between the cavity field and the mechanical oscillator, allowing efficient amplification of mechanical motion. A key challenge is that the strong dissipation leads to a short photon lifetime, whereas efficient optomechanical interaction demands a long one. We overcome this limitation by incorporating a Yb^{3+}-doped gain fiber, which provides high cavity finesse and tunable gain. This design maintains a stronger optomechanical coupling for coherent vibrational amplification. In this case, through increasing the power P of the pump laser (e.g., from 0 to 1.5 mW), the microsphere undergoes a phase transition from Brownian motion to sustained coherent oscillation, with a clear threshold between the two regimes (see Supplementary Note 3).

The trapping power is modulated via the diffraction effect of an acousto-optic modulator (AOM). We use the zero-order beam of the AOM for trapping microspheres, spatially filtering out the remaining diffraction orders. Within a certain range, the intensity of the electrical signal driving the AOM is proportional to the optical power of zero-order light. By applying a square wave to the AOM, non-adiabatic changes in the eigenfrequency of the microsphere oscillator can be induced, thereby enabling fully controllable and frequency-tunable phonon lasers. Based on this, we employ the squeezing protocol of non-adiabatic frequency shifts to generate squeezed nonlinear phonon lasers. For each parameter set, a sequence of 2500–3000 independent pulses with a 5 ms interval was performed. Taking the end of the pulse as time zero, a displacement value at time t was measured for each pulse, from which the corresponding variance was computed at a specific phase (See Supplementary Note 4 for more details).

A key characteristic of mechanical squeezing is that the noise is suppressed in the momentum quadrature while amplified in the position quadrature. The intensity of the noise is directly characterized by the variance, which measures the magnitude of the fluctuations in the mechanical oscillator. In our experiments, the degree of squeezing can be calculated from the ratio of the momentum noise variance before and after squeezing, given by the formula

$$\lambda_t = 10\log_{10}\left(\frac{\sigma_0^2}{\sigma_t^2}\right), \tag{3}$$

where $\sigma^2{}_0$ ($\sigma^2{}_t$) denotes the momentum noise variance of the phonon laser before (after) the squeezing pulse at a specific phase.

Microsphere trapping
Microspheres with a nominal diameter of 2μm were sourced from the China University of Petroleum. Prior to the experiments, the microspheres were cleaned by a centrifuge, and their concentration was maintained within an optimal range. Before being trapped under atmospheric pressure, they were loaded into the trapping region via an ultrasonic nebulizer. Subsequently, the pressure was reduced to the desired level (~20 mbar) for the experiments.

Phase-space distributions
To reconstruct the phase-space distribution of the microsphere reliably, an accurate determination of the momentum is indispensable. To achieve this, the temporal resolution of the detection system must be much shorter than the momentum relaxation time τ of the sphere, and the spatial resolution of the detection system must be much smaller than the displacement of the sphere during the measurement time[64]. The momentum relaxation time is related to the viscous damping factor, Γ_0, which is calculated from kinetic theory. Assuming that air molecules undergo diffuse reflection upon collision with the microsphere surface, and that the molecules thermally accommodate with the surface, we have:

$$\Gamma_0 = \frac{6\pi\eta R}{M}\frac{0.619}{0.619 + K_n}(1 + c_K), \tag{4}$$

where η is the viscosity coefficient of air, R denotes the radius of the microsphere, and M represents its mass. The Knudsen number is defined as $K_n = l / R$, where l is the mean free path of air molecules (calculated based on the actual composition of air). The function c_K, given by $c_K = (0.31K_n)/(0.785 + 1.152K_n + K^2{}_n)$, is a small positive correction term that depends on K_n. The momentum relaxation time was measured to be 165.6 μs for a 2-μm-diameter microsphere, with the Knudsen correction applied. The period of the fundamental mode was 56.2 μs. Both of these time scales are substantially longer than the temporal resolution of the displacement measurement (1 μs). Consequently, the momentum of the sphere can be directly estimated by computing the time derivative of its measured position. Using this approach, we mapped the phase-space distribution of the trapped microsphere's motion. Each phase-space plot consists of around 3000 scattered points (q_i, p_i), collected over repeated pulses.

Phonon correlations
To quantify the coherence of the mechanical oscillator, we use the normalized second-order correlation function with zero-time delay[65], defined as

$$g^{(2)}(0) = \frac{\left\langle \hat{b}^\dagger \hat{b}^\dagger \hat{b}\hat{b} \right\rangle}{\left\langle \hat{b}^\dagger \hat{b} \right\rangle^2} = \frac{\left\langle \hat{N}^2 \right\rangle - \left\langle \hat{N} \right\rangle}{\left\langle \hat{N} \right\rangle^2}, \tag{5}$$

where $\hat{N} = \hat{b}^\dagger \hat{b}$ denotes the phonon number operator and $\hat{b}(\hat{b}^\dagger)$ is the creation (annihilation) operator. The phonon number can be obtained from the view of the energy

$$\hat{H} = \frac{1}{2}\hbar\Omega_m\left(\Delta\hat{x}^2 + \Delta\hat{p}^2\right) = \hbar\Omega_m\left(\hat{b}^+\hat{b} + \frac{1}{2}\right) = \hbar\Omega_m\left(\hat{N} + \frac{1}{2}\right), \tag{6}$$

where $\left(\hat{b} + \hat{b}^\dagger\right)/\sqrt{2} = \Delta\hat{x} = \hat{x} - \langle\hat{x}\rangle$, $\left(\hat{b} - \hat{b}^\dagger\right)/i\sqrt{2} = \Delta\hat{p} = \hat{p} - \langle\hat{p}\rangle$, $\hat{p}(\hat{q})$ denotes the dimensionless position (momentum) operator[66]. With respect to the quadrature variables, the phonon number can be calculated by

$$\hat{N} = \frac{1}{2}\left(\Delta\hat{x}^2 + \Delta\hat{p}^2 - 1\right). \tag{7}$$

$g^{(2)}(0)$ serves as a key criterion to distinguish thermal motions ($g^{(2)}(0) = 2$) and coherent behaviors ($g^{(2)}(0) = 1$).

Error analysis
We investigated the ratio $\sigma^2{}_t/\sigma^2{}_0$and the normalized correlation function $g^{(2)}(0)$ (at zero-time delay) versus pulse duration τ and power ratio P_1/P_2. For each parameter set, the experiment was independently repeated 20 times. The data points represent the mean values from the repeated experiments, with the error bars indicating the standard deviation. Further detailed discussion of controls and mass calibration is provided in Supplementary Note 5.

Data availability
The data that support the plots within this paper have been deposited in the Figshare database under accession code [https://doi.org/10.6084/m9.figshare.32118982]. All other data used in this study are available from the corresponding authors.

Code availability
The computer codes that were used to generate the data that support the findings of this study are available from the corresponding authors.

References
1. Vahala, K. J. et al. A phonon laser. *Nat. Phys.* **5**, 682–686 (2009).

2. Sheng, J., Wei, X., Yang, C. & Wu, H. Self-organized synchronization of phonon lasers. *Phys. Rev. Lett.* **124**, 053604 (2020).
3. Pan, Z. et al. Ultra-stable phonon laser through closed-loop feedback control for optomechanical sensing. *Laser Photonics Rev.* **18**, 2400593 (2024).
4. Burgwal, R. & Verhagen, E. Enhanced nonlinear optomechanics in a coupled-mode photonic crystal device. *Nat. Commun.* **14**, 1526 (2023).
5. Vermeulen, S. M. et al. Direct limits for scalar field dark matter from a gravitational-wave detector. *Nature* **600**, 424–428 (2021).
6. Mirhosseini, M., Sipahigil, A., Kalaee, M. & Painter, O. Superconducting qubit to optical photon transduction. *Nature* **588**, 599–603 (2020).
7. Satzinger, K. J. et al. Quantum control of surface acoustic-wave phonons. *Nature* **563**, 661–665 (2018).
8. Jing, H. et al. PT -symmetric phonon laser. *Phys. Rev. Lett.* **113**, 053604 (2014).
9. Behrle, T. et al. Phonon laser in the quantum regime. *Phys. Rev. Lett.* **131**, 043605 (2023).
10. Jiang, Y., Maayani, S., Carmon, T., Nori, F. & Jing, H. Nonreciprocal Phonon Laser. *Phys. Rev. Appl.* **10**, 064037 (2018).
11. Lee, C.-Y., Lin, K.-T. & Lin, G.-D. Prototype of a phonon laser with trapped ions. *Phys. Rev. Res.* **5**, 023082 (2023).
12. Pettit, R. M. et al. An optical tweezer phonon laser. *Nat. Photonics* **13**, 402–405 (2019).
13. Kuang, T. et al. Nonlinear multi-frequency phonon lasers with active levitated optomechanics. *Nat. Phys.* **19**, 414–419 (2023).
14. Zhang, Q., Yang, C., Sheng, J. & Wu, H. Dissipative coupling-induced phonon lasing. *Proc. Natl. Acad. Sci.* **119**, e2207543119 (2022).
15. Kemiktarak, U., Durand, M., Metcalfe, M. & Lawall, J. Mode competition and anomalous cooling in a multimode phonon laser. *Phys. Rev. Lett.* **113**, 030802 (2014).
16. Zhang, J. et al. A phonon laser operating at an exceptional point. *Nat. Photonics* **12**, 479–484 (2018).
17. Chafatinos, D. L. et al. Polariton-driven phonon laser. *Nat. Commun.* **11**, 4552 (2020).
18. Wang, G. et al. Demonstration of an ultra-low-threshold phonon laser with coupled microtoroid resonators in vacuum. *Photonics Res.* **5**, 73 (2017).
19. Wang, N. et al. Laser^2: A two-domain photon-phonon laser. *Sci. Adv.* **9**, eadg7841 (2023).
20. Grudinin, I. S., Lee, H., Painter, O. & Vahala, K. J. Phonon Laser Action in a Tunable Two-Level System. *Phys. Rev. Lett.* **104**, 083901 (2010).
21. Cohen, J. D. et al. Phonon counting and intensity interferometry of a nanomechanical resonator. *Nature* **520**, 522–525 (2015).
22. Cui, K. et al. Phonon lasing in a hetero optomechanical crystal cavity. *Photonics Res.* **9**, 937 (2021).
23. Knünz, S. et al. Injection locking of a trapped-ion phonon laser. *Phys. Rev. Lett.* **105**, 013004 (2010).
24. Xiao, G. et al. Giant enhancement of nonlinear harmonics of an optical-tweezer phonon laser. *eLight* **4**, 17 (2024).
25. Bekker, C., Kalra, R., Baker, C. & Bowen, W. P. Injection locking of an electro-optomechanical device. *Optica* **4**, 1196 (2017).
26. Hossein-Zadeh, M. & Vahala, K. J. Observation of injection locking in an optomechanical oscillator. *Appl. Phys. Lett.* **93**, 191115 (2008).
27. Kuhn, S. et al. Optically driven ultra-stable nanomechanical rotor. *Nat. Commun.* **8**, 1670 (2017).
28. He, Y. et al. Coherent acoustic frequency comb via Floquet engineering of optical tweezer phonon lasers. *Sci. Adv.* **11**, eadv9984 (2025).
29. Mercadé, L. et al. Floquet Phonon lasing in multimode optomechanical systems. *Phys. Rev. Lett.* **127**, 073601 (2021).
30. Szorkovszky, A., Brawley, G. A., Doherty, A. C. & Bowen, W. P. Strong thermomechanical squeezing via weak measurement. *Phys. Rev. Lett.* **110**, 184301 (2013).
31. Youssefi, A., Kono, S., Chegnizadeh, M. & Kippenberg, T. J. A squeezed mechanical oscillator with millisecond quantum decoherence. *Nat. Phys.* **19**, 1697–1702 (2023).
32. Mashaal, A. et al. Strong thermomechanical noise squeezing stabilized by feedback. *Phys. Rev. Res.* **7**, L012071 (2025).
33. Lei, C. U. et al. Quantum nondemolition measurement of a quantum squeezed state beyond the 3 dB limit. *Phys. Rev. Lett*. (2016).
34. Rashid, M. et al. Experimental realization of a thermal squeezed state of levitated optomechanics. *Phys. Rev. Lett.* **117**, 273601 (2016).
35. Xin, M., Leong, W. S., Chen, Z., Wang, Y. & Lan, S.-Y. Rapid quantum squeezing by jumping the harmonic oscillator frequency. *Phys. Rev. Lett.* **127**, 183602 (2021).
36. Burd, S. C. et al. Quantum amplification of mechanical oscillator motion. *Science* **364**, 1163–1165 (2019).
37. Muffato, R. et al. Generation of classical non-Gaussian states by squeezing a thermal state into nonlinear motion of levitated optomechanics. *Phys. Rev. Res.* **7**, 013171 (2025).
38. Hu, X. & Nori, F. Phonon squeezed states: quantum noise reduction in solids. *Phys. B Condens. Matter* **263–264**, 16–29 (1999).
39. Hu, X. & Nori, F. Quantum phonon optics: coherent and squeezed atomic displacements. *Phys. Rev. B* **53**, 2419–2424 (1996).
40. Feng, Z. et al. Gain-enhanced suspended optomechanical system with tunable dissipative coupling strength. *Opt. Express* **32**, 34234 (2024).
41. Liška, V. PT-like phase transition and limit cycle oscillations in non-reciprocally coupled optomechanical oscillators levitated in vacuum. *Nat. Phys.* **20**, 1622–1628 (2024).
42. Reisenbauer, M. et al. Non-Hermitian dynamics and non-reciprocity of optically coupled nanoparticles. *Nat. Phys.* **20**, 1629–1635 (2024).
43. Serafini, A., Paris, M. G. A., Illuminati, F. & Siena, S. D. Quantifying decoherence in continuous variable systems. *J. Opt. B Quantum Semiclass. Opt.* **7**, R19–R36 (2005).
44. Lo, C. F. Squeezing by tuning the oscillator frequency. *J. Phys. A: Math. Gen.* **23**, 1155–1165 404 (1990).
45. Rossi, M. et al. Quantum delocalization of a levitated nanoparticle. *Phys. Rev. Lett.* **135**, 083601 (2025).
46. Agarwal, G. S. & Kumar, S. A. Exact quantum-statistical dynamics of an oscillator with time-dependent frequency and generation of nonclassical states. *Phys. Rev. Lett.* **67**, 3665–3668 (1991).
47. Janszky, J. & Yushin, Y. Y. Squeezing via frequency jump. *Opt. Commun.* **59**, 151–154 (1986).
48. Hu, X. & Nori, F. Squeezed phonon states: modulating quantum fluctuations of atomic displacements. *Phys. Rev. Lett.* **76**, 2294–2297 (1996).
49. Hu, X. & Nori, F. Phonon squeezed states generated by second-order Raman scattering. *Phys. Rev. Lett.* **79**, 4605–4608 (1997).
50. Qin, W., Kockum, A. F., Muñoz, C. S., Miranowicz, A. & Nori, F. Quantum amplification and simulation of strong and ultrastrong coupling of light and matter. *Phys. Rep.* **1078**, 1–59 (2024).
51. Kamba, M., Hara, N. & Aikawa, K. Quantum squeezing of a levitated nanomechanical oscillator. *Science* **389**, 1225–1228 (2025).
52. Qin, W., Miranowicz, A. & Nori, F. Beating the 3 dB limit for intracavity squeezing and its application to nondemolition qubit readout. *Phys. Rev. Lett.* **129**, 123602 (2022).
53. Xiao, K. et al. Q-switching of an optical tweezer phonon laser. *J. Phys. B Mol. Opt. Phys.* **55**, 245401 (2022).
54. Qin, W. & Nori, F. Enhanced interactions using quantum squeezing. *Physics* **17**, 64 (2024).
55. Aasi, J. et al. Enhanced sensitivity of the LIGO gravitational wave detector by using squeezed states of light. *Nat. Photonics* **7**, 613–619 (2013).
56. Pan, F. et al. Phonon lasing enhanced mass sensor with zeptogram resolution under ambient conditions. *Chip* **2**, 100050 (2023).

57. Feng, X. N., Zhang, M. & Wei, L. F. Beating the standard quantum limit electronic field sensing by simultaneously using quantum entanglement and squeezing. *Phys. Rev. Lett.* **132**, 220801 (2024).
58. Wei, Y.-Q. et al. Detection of DC electric forces with zeptonewton sensitivity by single-ion phonon laser. *Sci. China Phys. Mech. Astron.* **65**, 110313 (2022).
59. Ren, X. et al. Dual-comb optomechanical spectroscopy. *Nat. Commun.* **14**, 5037 (2023).
60. Tan, T. et al. Biomimetic acoustic perception via chip-scale dual-soliton microcombs. *eLight* **5**, 22 (2025).
61. Xiao, G. et al. Ultrabroadband phonon laser frequency comb. *Adv. Photonics* **8**, 220011 (2026).
62. Zhang, K., Xiao, K., Bhattacharya, M. & Vamivakas, A. N. A two-mode thermomechanically squeezed phonon laser. *Nat. Commun.* **17**, 2882 (2026).
63. Chen, Z. et al. Differential displacement measurement of the levitated particle using D-shaped mirrors in the optical tweezers. *Opt. Express* **30**, 30791 (2022).
64. Li, T., Kheifets, S., Medellin, D. & Raizen, M. G. Measurement of the instantaneous velocity of a Brownian particle. *Science* **328**, 1673–1675 (2010).
65. Glauber, R. J. The quantum theory of optical coherence. *Phys. Rev.* **130**, 2529–2539 (1963).
66. Li, G., Nie, W., Li, X. & Chen, A. Dynamics of ground-state cooling and quantum entanglement in a modulated optomechanical system. *Phys. Rev. A* **100**, 063805 (2019).

Acknowledgements
We gratefully acknowledge the valuable assistance from Qian Zhang at Hunan Normal University and Zijian Feng and Yutong He at the National University of Defense Technology.

Author contributions
G.X. and H.J. conceived the idea. X.S., G.L. and T.K. designed the experiments. X.S., G.L. and T.K. performed the experiments and analyzed the experimental data with the help of G.X., W.X., X.C., X.H. and Y.Z. T.K., G.L., X.S. and R.H. performed the theoretical analysis, guided by G.X. and H.J. X.S., G.L., T.K. and R.H. wrote the manuscript with contributions from G.X., H.J. and F.N. G.X., H.L. and H.J. supported the project.

Funding
This work was supported by the Quantum Science and Technology-National Science and Technology Major Project (2024ZD0301000), the National Natural Science Foundation of China (12474368, 12404420,11935006, 12421005), the Science Fund for Distinguished Young Scholars of Hunan Province (2024JJ2055), the Key Science and Technology Breakthrough Program of Hunan Province (2023ZJ1010), the National Key R&D Program (2024YFE0102400), the Hunan Major Sci-Tech Program (2023ZJ1010), the RIKEN Special Postdoctoral Researchers (SPDR) program, the Japan Science and Technology Agency (JST) [via the CREST Quantum Frontiers program (JPMJCR24I2), the Quantum Leap Flagship Program (Q-LEAP), and the Moonshot R&D (JPMJMS20611)].

Competing interests
The authors declare no competing interests.

Additional information
Supplementary information The online version contains supplementary material available at https://doi.org/10.1038/s41467-026-75601-9.

Correspondence and requests for materials should be addressed to Hui Jing, Hui Luo or Guangzong Xiao.

Peer review information *Nature Communications* thanks the anonymous reviewers for their contribution to the peer review of this work. A peer review file is available.